Bulletin of the Seismological Society of America, Vol. 97, No. 1B, pp. 114–127, February 2007, doi: 10.1785/0120060078

Chinese National Network Magnitudes, Their Relation to NEIC Magnitudes, and Recommendations for New IASPEI Magnitude Standards

by Peter Bormann, Ruifeng Liu, Xiao Ren, Rudolf Gutdeutsch, Diethelm Kaiser, and Silvia Castellaro

Abstract We investigate the linear regression relationships between common seismic magnitudes determined by the Chinese Earthquake Network Center (CENC) and compare them with related magnitude determinations for the same events at the U.S. Geological Survey's National Earthquake Information Center (NEIC). Despite their generally good agreement some systematic differences are revealed. These differences are due to differences in seismograph response (shape and bandwidth), the time window for measurement of maximum *P*-wave amplitudes, the period and distance ranges used, and, in part, also the different calibration functions applied. Chinese broadband body-wave magnitude m_B, compared with the NEIC short-period *P*-wave magnitude m_b, is much less prone to magnitude saturation. Thus it is more suitable to assess the size of large earthquakes from *P* waves. Also, following International Association of Seismology and Physics of the Earth's Interior (IASPEI) recommendations of 1967, Chinese surface-wave magnitude M_S is determined in a wider distance ($1° < \Delta < 180°$) and period range (3 sec $< T <$ 30 sec) than $M_S(20)$ at NEIC ($20° \leq \Delta \leq 160°$ and 18 sec $\leq T \leq$ 22 sec, respectively). Chinese M_S for small and medium earthquakes at regional distances between $2° < \Delta < 10°$ scales well with local magnitude M_L. In contrast, NEIC $M_S(20)$ tends to underestimate the magnitude of regional events when the IASPEI-recommended M_S calibration function by Vaněk *et al.* (1962) is used. These findings support some of the new standards for magnitude measurements from digital data adopted at the IASPEI meeting in 2005. They include, complementary to band-limited m_b and $M_S(20)$, the determination of m_B and M_S(BB) measured on unfiltered broadband records.

Introduction

Today a host of different magnitude scales exist that far exceed the limits of the original definition of earthquake magnitude by Richter (1935). Although most of them are somehow scaled to some reference value, they usually mean different things because they are based on the use of different wave types, different kinematic characteristics of the seismic wave field (ground displacement, velocity, or acceleration), measurements in different and often rather limited frequency ranges, either single-amplitude measurements or the integration of amplitudes within time windows of different length after the first wave onset, etc. The confusion among users of magnitude data is further complicated by the fact that for a given event not only the values reported by different agencies for different types of magnitudes (such as M_L, M_S, m_b, and M_w) sometimes deviate significantly, but also the values for the same kind of magnitude that are reported with identical nomenclature. A striking example is the m_b values determined by the National Earthquake Information Center (NEIC) of the U.S. Geological Survey (USGS) and the International Data Center (IDC; formerly PIDC and EIDC) under the Comprehensive Test-Ban Treaty Organization (CTBTO). According to Granville *et al.* (2002, 2005) the observed differences result primarily from the use of different response functions (Fig. 1). This is indeed one of the major factors, especially for smaller and medium events, and is considered by us in the following. However, the differences in the time windows applied at the IDC and NEIC, within which the maximum *P*-wave amplitude A_{max} is measured after the first *P* onset, seem to play an even larger role for greater events. The difference $\Delta m_b = m_b(\text{NEIC}) - m_b(\text{EIDC})$ shows strong magnitude dependence (Fig. 2). Δm_b grows from an average of $+0.06$ magnitude units (m.u.) for $m_b(\text{NEIC}) < 4.0$ to $+0.61$ m.u. for $m_b(\text{NEIC}) > 5.9$. For recent great earthquakes, such as the M_w 9.3 Sumatra Islands earthquake of 26 December 2004, it reached $+1.3$ m.u. (m_b(EIDC) 5.7 and m_b(NEIC) 7.0). When using simulated WWSSN short-period records (see Fig. 1 for instrument response) from 18 stations of the German Regional Seismic Network (GRSN) and measuring the largest *P*-wave amplitudes in the whole *P*-wave train (which arrived some 90 sec

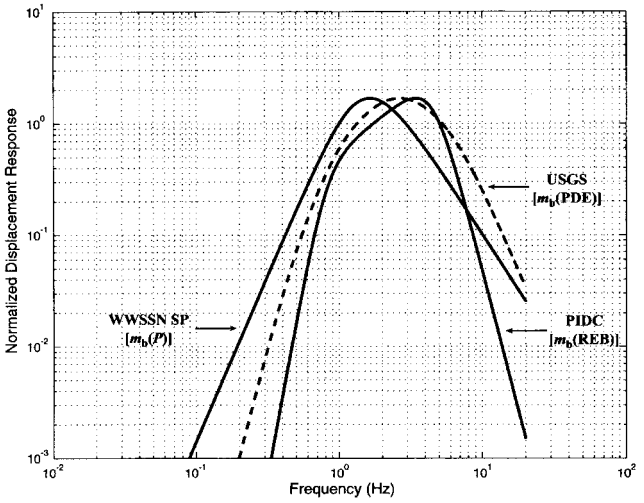

Figure 1. Normalized displacement responses of a typical WWSSN short-period instrument, the bandpass filtering applied by the USGS for its automatic PDE processing procedure, and the filtering according to the PIDC procedure for short-period data analysis. All responses are normalized to have the same peak gain (from Granville *et al.* [2005], p. 1813, Fig. 4, © Seismological Society of America).

and 350 sec after the first onset of *P*) one would get even an average of m_b 7.5 (Wendt, personal comm., 2005), that is, some 1.8 m.u. larger than m_b(EIDC).

Whereas the IDC measures A_{max} within 5.5 sec after the *P*-wave arrival (and CENC even within 5 sec), the NEIC measures usually within the first 10 *P*-wave cycles with an automatic procedure, and may later extend the window interactively up to 60 sec for the largest earthquakes (Granville *et al.*, 2005). The average rupture duration of earthquakes is <6 sec for moment magnitudes M_w 6, about 50 sec for M_w 7.5 and may last for several minutes for the strongest earthquakes (about 9 min for the M_w 9.3 Sumatra earthquake). Consequently, time windows for measuring A_{max} in the *P*-wave group that are shorter than the rupture duration, tend to underestimate m_b or m_B. We term this the time-window saturation component of body-wave magnitudes. It is more pronounced for m_b(EIDC) and m_b(CENC) than for m_b(NEIC). The other component is due to "spectral saturation" with respect to the seismic scaling law (Aki, 1967). All band-limited magnitude data show spectral saturation. It is less pronounced for long-period magnitudes and absent for "zero-frequency" M_w (Kanamori, 1983). Short-period m_b estimates that are based on displacement amplitude measurements at periods typically $T < 2$ sec, will already underestimate the true size of events whose source spectra have corner periods $T_c > 2$ sec. For "average earthquakes" this is the case for moment magnitudes M_w >5–6 because then $(A/T)_{max}$ is no longer measured at frequencies of maximum seismic moment rate release but on the decaying slope of the seismic source spectrum (Bormann *et al.*, 2002, Figures 3.5 and 3.18). The higher the upper-corner frequency (with peak magnification) and the narrower the relative bandwidth of the record filter (cf. Fig. 1), the earlier a magnitude derived from such a record will begin to saturate. Note that record amplitudes scale with the square root of the relative bandwidth (Bormann, 2002b). Thus, the systematic and magnitude-dependent differences between m_b(NEIC) and m_b(EICD) (but also m_b(CENC), as shown later) will become understandable. For M_w <6 they are mainly due to differences in the frequency responses used and thus different spectral saturation, whereas for larger magnitudes differences in the measurement time windows may become dominant.

Although m_b, by its very nature, systematically underestimates the overall size of large earthquakes, it allows a rather quick and realistic assessment of the amount of high-frequency energy released by an earthquakes and thus of its potential to cause shaking damage. However, inconsistent practices and thus incompatible values published by different agencies may be misleading and prevent the use of m_b, in combination with M_w and other types of magnitudes, for a more realistic assessment of the actual seismic hazard. Therefore, the International Association of Seismology and Physics of the Earth's Interior (IASPEI) entrusted in 2001 an international Working Group (WG) on Magnitudes with the task to propose standards for making measurements from digital data for widely catalogued and commonly used body- and surface-wave magnitudes with the aim to reduce existing systematic inconsistencies and biases, which still limit the value of such magnitude data both for research and practical application.

The following study has been carried out in the framework of that WG in which two authors (P.B. and L.R.) are regular members. It is based on magnitude data for M_L, m_b, m_B, M_S, and M_{S7}, which are routinely determined at the China Earthquake Network Center (CENC), not, however, M_w. CENC uses for its national catalog only the records from 92 so-called first- and second-class stations within China. These data are compared among each other and subsequently with the teleseismic magnitudes m_b and M_S determined at NEIC, which are based on records from a global station network. The analysis is based on linear regression relations between different pairs of magnitudes. Systematic deviations are discussed in terms of differences in the instrument response, wave type, length of time window for amplitude measurements, and calibration function used, because these parameters have been rather stable at both agencies over the considered time span of 25 years. We do not consider differences in network configuration and number of seismic stations used to determine event magnitudes for different source regions. They are subject to changes with time and event magnitude itself. Also, as discussed in Bormann *et al.* (2002, section 3.2.7), global relationships between different types of teleseismic magnitudes determined from single-station and worldwide network records, respectively, scale rather well, provided that the same waves, instrument types, and measurement procedures have been applied.

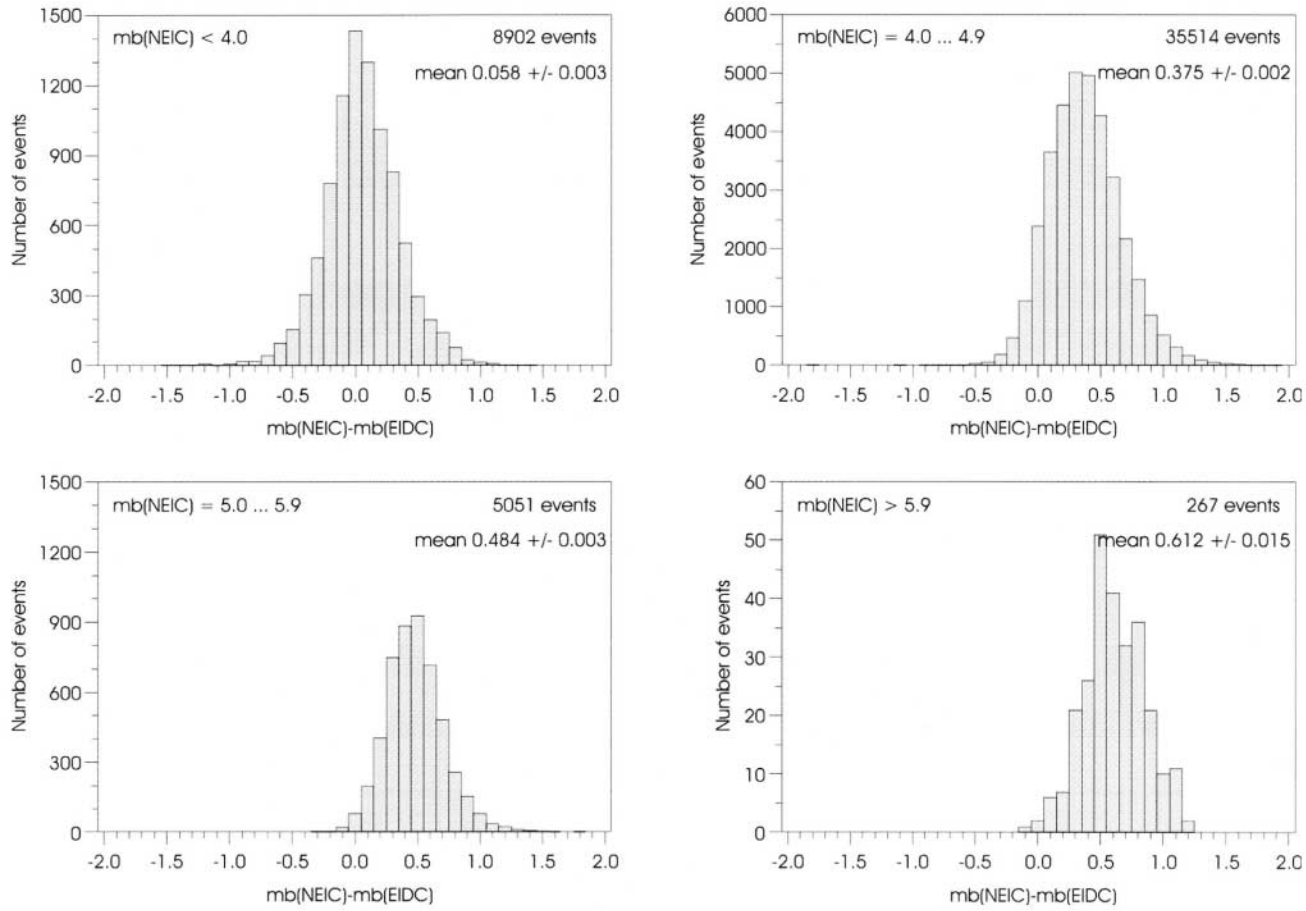

Figure 2. Differences in m_b for events reported by NEIC and the EIDC of the CTBTO between the years 1995 and 2000 (courtesy of S. Wendt, 2003).

In this article we use the generic magnitude nomenclature (italics with subscripts) common in *BSSA*. In the figure annotations, however, we preferred the simpler corresponding nomenclature without subscripts used in the IASPEI New Manual of Seismological Observatory Practice (NMSOP; Bormann, 2002a) as standard for international data exchange and cataloguing. The Chinese magnitudes are presented—for reasons of brevity—with nonextended generic magnitude symbols, although CENC magnitudes are not yet fully compatible with the envisaged new standards. To differentiate Chinese magnitudes from related NEIC magnitudes, we add (NEIC) to the latter.

Seismometer Parameters and Magnitude Formulas Used

NEIC magnitude data have been taken from the Preliminary Determination of Epicenter (PDE). Whereas the original seismic records are nowadays commonly velocity proportional broadband records, the magnitude measurements for m_b are made on records with a simulated short-period response (see curve USGS [m_b(PDE)] in Fig. 1) and for M_S with a simulated long-period WWSSN seismograph response, respectively (identical with response 763 in Fig. 3). On such band-limited records A_{max} is measured from P waves with periods $T < 3$ sec for m_b(NEIC) and from surface waves with periods $T = 20 \pm 2$ sec for calculating M_S(NEIC). The time window for measuring A_{max} of P waves was explained in the introduction. For calibrating the short-period m_b, NEIC uses the Q-values published by Gutenberg and Richter (1956) for vertical component *PZ* waves, although these authors had mainly used medium- to long-period records from rather broadband instruments to derive their body-wave calibration values. M_S magnitudes are calibrated at NEIC with the $\sigma(\Delta)$-function published by Vaněk *et al.* (1962) in the epicentral distance range $20° \leq \Delta \leq 160°$, although this function had been developed for application in a wide range of periods (3 sec $< T <$ 60 sec) and distances ($2° < \Delta < 160°$). The averaged function $\sigma(\Delta) = 1.66 \log(\Delta) + 3.3$ was adopted by IASPEI in 1967 as the international standard for M_S determination. One has to be aware, however, that the calibration of band-limited 20 sec surface-wave amplitude readings with this broadband calibration function results in systematic distance-dependent biases of $M_S(20)$. This led Herak and Herak (1993) and Rezapour and Pearce (1998) to propose improved $M_S(20)$

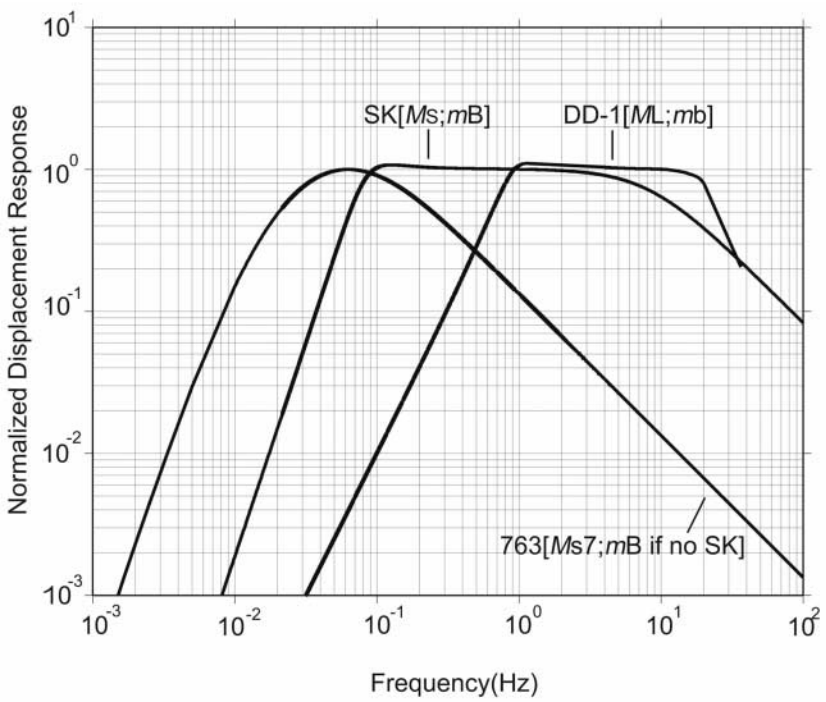

Figure 3. Normalized displacement responses of the three standard types of seismographs used in the Chinese network until 2001. Presently, these responses are simulated from digital broadband records for magnitude measurements. The types of magnitudes determined from these records are given in brackets.

calibration functions, which, however, have not yet been introduced as new international standards for $M_S(20)$ magnitudes.

Seismometer parameters, measurement procedures, and magnitude formulas used in the China Seismic Network are slightly different from those used at NEIC. The catalog phase data and event waveforms of the China National Network used in this study are available on-line. The waveforms are in SEED format. At present, however, this website (www.csndmc.ac.cn) exists in Chinese only. An English version will be available soon. Until 31 December 2001, records and analysis procedures were analog. Since 1 January 2002, the CENC switched to digital broadband records and analysis tools. Although Chinese m_B and M_S data have been available since 1979, M_L, m_b, and M_{S7} have been regularly determined since 1983, 1988, and 1989, respectively. Comparisons between CENC and NEIC magnitudes up to 31 December 2004 have been made for M_S-m_b(NEIC) and M_S-M_S(NEIC) since 1983, for m_B-M_S(NEIC) since 1985, for m_b-m_b(NEIC) since 1988, and for M_{S7}-m_b(NEIC) and M_{S7}-M_S(NEIC) since 1989.

Figure 3 depicts the normalized amplitude-frequency responses of seismic records used up to now as standards for magnitude determination. The respective analog seismographs had the following seismometer (T_s) and galvanometer/pen-recorder eigenperiods (T_g) and dampings (D_s and D_g), respectively:

DD-1: $T_s = 1.0$ sec, $T_g = 0.05$ sec,
$D_s = 0.45$ and $D_g = 0.707$

SK: $T_s = 12.5$ sec, $T_g = 1.20$ sec,
$D_s = 0.45$ and $D_g = 5.0$

763: $T_s = 15.0$ sec, $T_g = 100.0$ sec,
$D_s = 1.0$ and $D_g = 1.0$

The response shape of DD-1 resembles that of the short-period Wood–Anderson seismograph, the SK response corresponds to the classical Russian medium-period Kirnos seismograph, and the response of 763 is equivalent to that of the WWSSN long-period seismograph. Simulation filters are now applied in the digital analysis procedures to reproduce the preceding responses from broadband records, thus assuring compatibility of old and modern magnitude estimates and long-term catalog homogeneity. The seismograph responses and the poles and zeros of the simulation filters used for producing the standard responses are accessible via www.csndmc.ac.cn (Chinese and English versions). The following response types and magnitude formulas are used for the various types of Chinese magnitudes.

Local magnitude M_L is computed from (simulated) DD-1 records by employing the calibration values $R(\Delta)$ derived for Beijing Station on the basis of DD-1 records:

$$M_L = \log(\bar{A}) + R(\Delta) \quad (0 \text{ km} < \Delta < 1000 \text{ km}), \quad (1)$$

where $\bar{A}$ is the average value of the horizontal ground displacement $\bar{A} = (An + Ae)/2$ with An the maximum ground displacement amplitude in the record of the north–south and Ae that of the east–west component in micrometers. An and Ae may not occur at the same times. The calibration values $R(\Delta)$, given in Table 1, correspond to Chinese crustal conditions, but they are tied at 90–100 km epicentral distance to the original values given by Richter (1935) for California.

Surface-wave magnitudes are determined in two different ways—M_S and M_{S7}. M_S is computed from (simulated) SK records by employing the 1965 formula of Beijing Station (see Guo and Pang, 1981):

$$M_S = \log(A/T)_{max} + \sigma(\Delta). \quad (2)$$

A is the resultant (vectorially combined) maximum long-period horizontal ground-motion displacement amplitude $A_H = (A_N^2 + A_E^2)^{1/2}$ in micrometers and T (in seconds) the surface-wave period at this maximum amplitude. Measurements are made at two to three different amplitude maxima so as to be sure to use equation (2) with the real $(A/T)_{max}$ in the considered period range 3 sec $\leq T \leq$ 25 sec. For earthquakes with source depth $h < 80$ km, the following calibration functions are applied:

$$\sigma(\Delta) = 1.66 \log(\Delta) + 3.5 \quad \text{for } 1^\circ < \Delta < 130^\circ \quad (3)$$

and

$$\sigma(\Delta) = 6.775 + \frac{1}{2}\left[(2.147 \exp(-0.04465\Delta + 1.325)(\Delta - 90) \times 10^{-2} + \log \sin \Delta + \frac{1}{3}(\log \Delta - 1.954)\right] \quad \text{for } 130^\circ < \Delta < 180^\circ. \quad (4)$$

Equations (3) and (4) follow exactly the structure of the original Gutenberg (1945) calibration function for surface waves in the same distance intervals, but with the coefficients and constants adapted by Guo and Pang (1981) to the response characteristic of the SK instrument used in China for M_S determination. However, in routine record analysis of the China National Network, M_S is determined only in the range $1^\circ < \Delta < 130^\circ$ by using equation (3). It resembles the $\sigma(\Delta) = 1.66 \log(\Delta) + 3.3$ proposed by Vaněk *et al.* (1962), but (3) yields +0.2 m.u. larger values. M_S calculation based on equation (4) is limited to research work.

A different surface-wave magnitude M_{S7} is computed from records of a Chinese-made long-period seismograph of type 763 by employing the formula:

$$M_{S7} = \log(A/T)_{max} + \sigma(\Delta)_{763} \quad \text{for } 3^\circ < \Delta < 177^\circ. \quad (5)$$

The calibration function $\sigma(\Delta)_{763}$ has been developed on the basis of data from Chinese stations. It is applicable to earthquakes with source depth $h < 50$ km in the given range of Δ. A is the maximum long-period surface-wave displacement on the vertical component (A_Z) with periods $T > 6$ sec. Between 20° and 160° $\sigma(\Delta)_{763}$ is identical with the IASPEI calibration function $\sigma(\Delta) = 1.66 \log(\Delta) + 3.3$. Between 3° and 20° and from 160° to 177°, $\sigma(\Delta)_{763}$ differs slightly from $\sigma(\Delta)$. Table 2 summarizes $\sigma(\Delta)_{763}$ values as a function of Δ.

Body-wave magnitudes are determined in two different ways by the formula:

$$m_b \text{ or } m_B = \log(A/T)_{max} + Q(\Delta, h) \quad (6)$$

with the Gutenberg–Richter (1956) calibration values $Q(\Delta, h)$ for vertical component P and PP waves, respectively. CENC calculates m_b and m_B for P waves between $5^\circ < \Delta \leq 100^\circ$ and also m_B (about 10% of all m_B data) for PP waves between $100^\circ < \Delta \leq 170^\circ$. For m_b $(A/T)_{max}$ is measured from the DD-1 (filtered) records for periods $T \leq 3$ sec and within a time window of only 5 sec after the P-wave first onset, while m_B is usually determined from intermediate period SK or long-period 763 record if no SK records are available. The time window applied at CENC for measuring $(A/T)_{max}$ for m_B determination follows the recommendations in the Manual of Seismological Observatory Practice (Willmore, 1979), namely measuring $(A/T)_{max}$ usually within 20 sec, and for large earthquakes within 60 sec after the P-wave first onset.

Table 1
Calibration Function $R(\Delta)$ for Chinese Local Magnitude M_L

Epicentral Distance Δ (km)	R(Δ)	Epicentral Distance Δ (km)	R(Δ)	Epicentral Distance Δ (km)	R(Δ)
0–5	1.8	55	3.1	290–320	4.1
10	1.9	60–70	3.2	330–340	4.2
15	2.0	80–85	3.3	350–390	4.3
20	2.1	90–100	3.4	400–460	4.4
25	2.3	110–140	3.5	470–600	4.5
30	2.5	150–160	3.6	610–650	4.6
35	2.7	170–200	3.7	700–800	4.7
40	2.8	210–220	3.8	850–900	4.8
45	2.9	230–260	3.9	1000	
50	3.0	270–280	4.0		

The $R(\Delta)$ values are valid for the preceding epicentral distance values and are linearly interpolated for Δ values in between.

Table 2
The Calibration Function $\sigma(\Delta)_{763}$.

Δ°	σ(Δ)	Δ°	σ(Δ)	Δ°	σ(Δ)	Δ°	σ(Δ)
3	4.48	45	6.04	90	6.54	135	6.86
5	4.81	50	6.11	95	6.59	140	6.89
10	5.13	55	6.18	100	6.63	145	6.93
15	5.34	60	6.24	105	6.65	150	6.96
20	5.51	65	6.30	110	6.69	155	6.98
25	5.65	70	6.35	115	6.72	160	6.99
30	5.77	75	6.40	120	6.76	165	6.98
35	5.87	80	6.45	125	8.79	170	6.94
40	5.96	85	6.50	130	6.82	175	6.83
						177	6.62

The $\sigma(\Delta)$ values are valid for the preceding epicentral distance values Δ° and are linearly interpolated for Δ° values in between.

Regression Relations

Linear regression

$$y = Ax + B \tag{7}$$

is commonly used to study the relationships between different magnitude data and to derive formulas to convert one type of magnitude into another one. The underlying assumption is that the compared magnitudes scale linearly. When comparing magnitudes based on the same wave types, using similar measurement procedures and working in comparable period ranges, then linear regression analysis is in general a viable approach. The comparison of magnitudes determined in very different period ranges, such as m_b and M_S, with m_b showing strong saturation, would instead require nonlinear regression analysis. However, the aim of this article is not to derive the most accurate conversion relationships between Chinese and NEIC magnitudes but to assess their compatibility, to look for systematic differences, and to identify possible reasons for these differences. When they are significant, they will also show up in a nonoptimal linear regression.

Most of the published regression relations between magnitudes, like the classical relations between m_B, M_S, and M_L by Gutenberg and Richter (1956), have been determined through linear standard least-squares regression (SR). SR provides the A and B parameters of the best-fitting linear equation (7) under the assumption that initial errors, for example, measurement errors, on one variable are much larger than on the other, that they are normally distributed and constant in the regression domain (Draper and Smith, 1998). Two cases are thus possible (with σ^2_{xxi} and σ^2_{yyi} = variances of the ith element of x_i and y_i and both $\sigma^2_{xxi} = \sigma^2_{xx}$ and $\sigma^2_{yyi} = \sigma_{yy}$ being constant):

1. SR1 with $\sigma^2_{xx} = 0$ and $\sigma^2_{yy} > 0$ follows from error equation

$$v_i^{(1)} = y_i^{(1)} - A_1 x_i - B_1,$$

which, by minimizing the square sum of $v_i^{(1)}$, leads to the well-known prescription

$$y_i^{(1)} \leftarrow A_1 x_i + B_1$$

The symbol "←" means that the relation holds only from right to left.

2. SR2 with $\sigma^2_{xx} > 0$ and $\sigma^2_{yy} = 0$ follows from the error equation

$$v_i^{(2)} = x_i^{(2)} - A_2' y_i - B_2',$$

$$x_i^{(2)} \leftarrow A_2' y_i + B'.$$

Applied to magnitudes, this implies that SR1 or SR2 can be used only when either M_y or M_x, respectively, are affected by errors. Users of published magnitude standard regressions are often not aware of it and resolve the regression prescription for the other variable. However, on noisy magnitude data sets, SR1 and SR2 may lead to differences in results of more than 1 m.u. (Bormann and Khalturin, 1975; Bormann *et al.*, 2002, section 3.2.7; see also Figs. 5 and 6 in the following). When incorrectly interpreted in seismic-hazard and energy-release studies this may have detrimental consequences (Castellaro *et al.*, 2006). Therefore, in Tables 3 and 4 we give the SR1 and SR2 relations with arrows. However, one has to consider that SR1 projects any error in M_x to M_y, and SR2 vice versa, thus increasing the uncertainty of the estimated dependent variable. The difference between A_1 and $A_2 = 1/A_2'$ can be regarded as a measure of the uncertainty of such conversions.

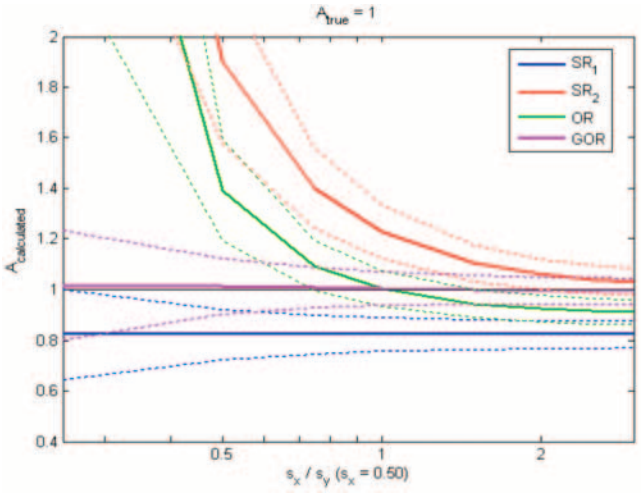

Figure 4. Calculated A values ($A_{calculated}$) as function of the error ratio s_x/s_y for fixed $s_x = 0.5$ depending on the type of regression analysis (SR1, SR2, OR, or GOR) applied to the data. The calculations are based on randomly generated 10^3 sets of 10^2 couples of magnitudes M_x and M_y in the interval $3.5 \le M \le 9.5$, assuming that, on average between the two magnitudes, a linear relationship exists in the form $M_y = M_x + B$, that is, with a true slope $A_{true} = 1$. The average $A_{calculated}$ values resulting from the different regression procedures are shown by the thick colored lines, their related standard deviations by the dotted lines. For details on methodology and results see Castellaro and Bormann (2006).

Best-fitting linear regressions procedures for variable initial errors on the variables provides the χ^2-regression. Stromeyer *et al.* (2004) used it for seismological problems. The so-called general orthogonal regression (GOR) (e.g., Fuller, 1987; Carroll and Ruppert, 1996; Castellaro *et al.*, 2006) include a special case of the χ^2-regression with initial errors $s_{xi} = s_x = \text{const1}$, $s_{yi} = s_y = \text{const2}$. However, its application requires knowing, at least approximately, the initial error ratio s_x/s_y. For magnitudes this is usually not known *a priori*. The common assumption that magnitude data of the same type have errors of the same size leads then to the

Table 3
Relationships between Chinese Magnitudes

M_x-M_y N	Regression	Relationship	rms Error	Figure
m_B-m_b	SR1	$m_b \leftarrow 0.72m_B + 1.23$	±0.24	
	SR2	$m_B \leftarrow 1.02m_b + 0.16$	±0.28	5, middle left
20,647	OR	$0.55 = -0.63m_B + 0.77\ m_b$	±0.19	
M_L-m_b	SR1	$m_b \leftarrow 0.45M_L + 2.47$	±0.31	
	SR2	$M_L \leftarrow 0.90m_b + 0.35$	±0.43	5, upper left
7,024	OR	$1.60 = -0.51M_L + 0.86m_b$	±0.27	
M_L-m_B	SR1	$m_B \leftarrow 0.57M_L + 2.27$	±0.37	
	SR2	$M_L \leftarrow 0.73m_B + 1.09$	±0.42	
2,485	OR	$0.82 = -0.64M_L + 0.77m_B$	±0.30	
M_s-M_L	SR1	$M_L \leftarrow 0.79M_s + 0.95$	±0.35	
	SR2	$M_s \leftarrow 0.80M_L + 0.83$	±0.36	5, upper right
7,851	OR	$0.05 = -0.70M_s + 0.71M_L$	±0.27	
M_{S7}-M_L	SR1	$M_L \leftarrow 0.79M_{S7} + 1.08$	±0.38	
	SR2	$M_{S7} \leftarrow 0.72M_L + 1.01$	±0.37	
5,500	OR	$-0.04 = -0.73M_{S7} + 0.68M_L$	±0.28	
M_s-m_b	SR1	$m_b \leftarrow 0.54M_s + 2.30$	±0.29	
	SR2	$M_s \leftarrow 1.15m_b - 0.79$	±0.42	
24,552	OR	$1.61 = -0.53M_s + 0.85m_b$	±0.25	
M_s-m_B	SR1	$m_B \leftarrow 0.67M_s + 1.98$	±0.30	
	SR2	$M_s \leftarrow 1.07m_B - 0.63$	±0.38	
19,104	OR	$1.21 = -0.60M_s + 0.80m_B$	±0.25	
M_{S7}-m_b	SR1	$m_b \leftarrow 0.54M_{S7} + 2.43$	±0.28	
	SR2	$M_{S7} \leftarrow 1.17m_b - 0.95$	±0.40	5, lower left
25,791	OR	$1.72 = -0.53M_{S7} + 0.85m_b$	±0.24	
M_{S7}-m_B	SR1	$m_B \leftarrow 0.66M_{S7} + 2.13$	±0.29	
	SR2	$M_{S7} \leftarrow 1.07m_B - 0.87$	±0.37	5, lower right
16,394	OR	$1.35 = -0.60M_{S7} + 0.80m_B$	±0.24	
M_s-M_{S7}	SR1	$M_{S7} \leftarrow 0.94M_s + 0.06$	±0.18	
	SR2	$M_s = 0.98M_{S7} + 0.28$	±0.19	5, middle right
25,002	OR	$-0.08 = -0.70M_s + 0.71M_{S7}$	±0.13	

N, number of values.

use of the simpler orthogonal regression (OR), which is the best-fitting linear regression when the initial error ratio $s_x/s_y = 1$. OR yields a linear equation $y = A_3\ x + B_3$. If the condition $s_x/s_y = 1$ is sufficiently met, which is the case for $0.7 \leq s_x/s_y \leq 1.5$, OR allows more reliable conversions than SR1 or SR2 (Fig. 4). For further details see Castellaro and Bormann (unpublished manuscript, 2006) and Gutdeutsch *et al.* (2005).

In Tables 3 and 4 we present all our results on Chinese and NEIC magnitude relationships as SR1 in the form $y \leftarrow A_1\ x + B_1$, as SR2 in the form of $x \leftarrow (y - B_2)/A_2$ and as OR in Hesse's normal form, where both variables appear on the right side:

$$p = n_x\ x + n_y\ y, \tag{8}$$

with p = orthogonal distance of the slope from the origin, $(n_x, n_y) = n_i$ = unit vector in the origin, perpendicular to the slope.

The orthogonal error v_i of data x_i, y_i follows from (8) by

$$v_i^{(3)} = p - n_x\ x_i - n_y\ y_i \tag{9}$$

as a linear combination of both x_i and y_i, weighted by the factors n_x and n_y. It does not derive from standard regression, and equations (8) and (9) can thus be resolved for both variables if the condition $s_x/s_y \approx 1$ holds. Accordingly, we can write the orthogonal regression

$$y^{(3)} = A_3\ x^{(3)} + B_3 \tag{10}$$

as a reversible equation with $p = B_3/q$, $n_x = -A_3/q$, $n_y = 1/q$, $q = (1 + A_3^2)^{1/2}$ and $-n_x/n_y = A_3$. In agreement with theory it holds (see Figs. 5 and 6) that

$$A_1 < A_3 < A_2. \tag{11}$$

Table 4
Relationships between NEIC and Chinese Magnitudes

M_x-M_y N	Regression	Relationship	rms Error	Figure
M_s(NEIC)-m_b(NEIC)	SR1	m_b(NEIC) ← 0.48M_s(NEIC) + 2.84	± 0.26	
	SR2	M_s(NEIC) ← 1.28m_b(NEIC) − 1.70	± 0.42	6, lower left
18,074	OR	2.22 = −0.47M_s(NEIC) + 0.88m_b(NEIC)	± 0.24	
M_s(NEIC)-m_b	SR1	m_b ← 0.44M_s(NEIC) + 2.97	± 0.25	
	SR2	M_s(NEIC) ← 1.30m_b − 1.76	± 0.44	
12,842	OR	2.40 = −0.45M_s(NEIC) + 0.89m_b	± 0.23	
M_s(NEIC)-m_B	SR1	m_B ← 0.57M_s(NEIC) + 2.67	± 0.25	
	SR2	M_s(NEIC) ← 1.24m_B − 1.83	± 0.37	6, lower right
10,756	OR	1.98 = −0.54M_s(NEIC) + 0.84m_B	± 0.21	
M_s-m_b(NEIC)	SR1	m_b(NEIC) ← 0.56M_s + 2.19	± 0.32	
	SR2	M_s ← 1.06m_b(NEIC) − 0.32	± 0.44	
30,984	OR	1.39 = −0.56M_s + 0.83m_b(NEIC)	± 0.27	
M_{S7}-m_b(NEIC)	SR1	m_b(NEIC) ← 0.57M_{S7} + 2.25	± 0.31	
	SR2	M_{S7} ← 1.03m_b(NEIC) − 0.40	± 0.41	
26,819	OR	1.42 = −0.57M_{S7} + 0.82m_b(NEIC)	± 0.26	
M_s-M_s(NEIC)	SR1	M_s(NEIC) ← 0.95M_s + 0.05	± 0.30	
	SR2	M_s ← 0.85M_s(NEIC) + 0.99	± 0.28	6, middle left
14,808	OR	−0.38 = 0.73M_s − 0.69M_s(NEIC)	± 0.21	
M_{S7}-M_s(NEIC)	SR1	M_s(NEIC) ← 0.98M_{S7} + 0.06	± 0.24	
	SR2	M_{S7} ← 0.88M_s(NEIC) + 0.63	± 0.23	6, middle right
13,107	OR	−0.23 = −0.73M_{S7} + 0.69M_s(NEIC)	± 0.17	
m_b-m_b(NEIC)	SR1	m_b(NEIC) ← 0.97m_b + 0.13	± 0.25	
	SR2	m_b ← 0.77m_b(NEIC) + 1.14	± 0.22	6, upper left
44,523	OR	−0.47 = −0.75m_b + 0.66m_b(NEIC)	± 0.17	
m_B-m_b(NEIC)	SR1	m_b(NEIC) ← 0.77m_B + 0.98	± 0.25	
	SR2	m_B ← 0.95m_b(NEIC) + 0.50	± 0.28	6, upper right
23,676	OR	0.28 = −0.66m_B + 0.75m_b(NEIC)	± 0.20	

N, number of values.

To verify whether OR can be used as an (at least near) optimal regression for our data, where $s_x/s_y \approx 1$ is expected, we analyzed a test data set. It has been randomly selected from the CENC database, which covers events in a wide range of teleseismic distances and magnitudes ($4 < M_s < 9$). We determined the average network magnitudes and the root-mean-square (rms) deviation of individual station magnitudes from the network averages. The rms values for individual earthquakes showed no distinct magnitude or distance dependence. Therefore, for different types of magnitudes, we calculated the average rms_{av} over the whole considered magnitude and distance range together with the standard deviation of the individual event rms with respect to the average rms_{av}. We got the following: m_b 0.35 ± 0.09, m_B 0.28 ± 0.06, M_S 0.23 ± 0.07; M_{S7} 0.26 ± 0.10. Accordingly, short-period China m_b has the largest rms_{av}, about 1.3 to 1.5 times larger than for long-period and broadband magnitudes, whereas the average error ratio for the latter is close to 1 (≤1.2). For such error ratios and $rms_{av} \leq 0.25$ m.u. the absolute differences between A_{GOR} and $A_{OR} = A_3$ will be much smaller than those shown in Figure 4. Accordingly, the average conversion errors due to OR instead of χ^2-regression will be <0.1–0.2 m.u. everywhere in the whole considered magnitude range between $3 < M < 9$. Regrettably, NEIC does not currently publish an estimate of magnitude standard deviation from the mean event magnitudes (J. Dewey, personal comm. 2006). Therefore, we can only assume similar errors and error ratios for NEIC magnitudes and expect OR to be very close to optimal linear regression also when comparing CENC and NEIC magnitudes (See Fig. 6). In general, we recommend the use of OR as a standard procedure for comparing and judging the relationship of magnitude data produced by different agencies as long as no quantified error data for both variables are available that allow the use of the optimal χ^2-regression. (The software is available by request to d.kaiser@bgr.de.)

Regression Relations between Chinese and NEIC Magnitudes

In Figure 5 we present diagrams of the most relevant *x*-*y* relations for the following pairs of Chinese magnitudes: M_L-m_b, M_S-M_L, m_B-m_b, M_S-M_{S7}, M_{S7}-m_b, and M_{S7}-m_B. The related regression formulas are given in Table 3, and

also for the additional relations M_L-m_B, M_{S7}-M_L, M_S-m_b, and M_S-m_B.

The Chinese teleseismic m_b, m_B, M_S, and M_{S7} are then compared with m_b(NEIC) and M_S(NEIC; 20 ± 2 sec) in the following *x*-*y* combinations: m_b-m_b(NEIC), m_B-m_b(NEIC), M_S-M_S(NEIC), M_{S7}-M_S(NEIC), M_S(NEIC)-m_b(NEIC), and M_S(NEIC)-m_B (Fig. 6). Their regression formulas, together with those for M_{S7}-m_b(NEIC), M_S(NEIC)-m_b, are given in Table 4. To assure that magnitudes for identical events are compared, the following procedure has been applied: CENC and NEIC exchange their event catalog and phase-pick data every month. For events in China or neighboring countries, the CENC catalog is used as a reference to associate the *P*-phase pick data of NEIC with the CENC event catalog. If most *P* arrivals have residuals <5 sec, then it is assumed that the two events compared in both catalogs are the "same." For events outside China and its neighboring countries no events with magnitudes smaller than 5 or 5.5 have been used in our data set. For those larger and less-frequent events it is not difficult to find the same event in both bulletins on the basis of the travel-time residual criterion. The amount of data available for each considered magnitude pair ranges between 7024 and 44,523. The data density per grid point varies from 1 up to more than 1000 data points. To illustrate the large differences in data density per grid point nine color-coded data frequency classes have been defined with geometrically increasing class width, because the precision of a statistical solution improves with $\sqrt{N}$.

Comments on the Chinese Regression Relations

Comments on the regression relations depicted in Figure 5 are summarized in this section (from left to right and downward):

M_L-m_b

Chinese m_b is determined in the whole distance range for which calibration values $Q(\Delta,h)_{PZ}$ have been given by Gutenberg and Richter (1956), that is, down to epicentral distance 5°, in contrast to NEIC, which minimizes the use of $Q(\Delta,h)$ for distances less the 21°. Therefore, Chinese m_b can be correlated with M_L between $3 \le M_L \le 7$. Yet, the scatter is the largest of all studied relations because of the large uncertainties in $Q(\Delta,h)_{PZ}$ for distances <20°, where wave propagation is strongly effected by upper-mantle, low-velocity zones and crustal inhomogeneities. Experience gained at NEIC shows that m_b determined from regional data tends to be systematically higher than teleseismic m_b for many parts of the Earth (J. Dewey, personal comm., 2006). This might explain the obvious m_b outliers, for example, in the M_L range between 3 to 4, with m_b values between 4.8 and 5.5. Thus, our results do not encourage the routine use of regional m_b, yet a systematic investigation of such m_b anomalies and their causes is suggested.

M_S-M_L

Chinese M_S is also determined in the distance range $1° < \Delta < 10°$ and available for magnitudes $2.5 \le M_S \le 7.5$. In contrast to M_L-m_b, M_S-M_L has a much larger correlation coefficient and an ideal OR slope of 1. This illustrates the usefulness and compatibility of local and regional M_S determinations in China.

m_B-m_b

This relation has a high correlation coefficient and rather low orthogonal root-mean-square error (RMSO). However, for m_B >4.5, m_b tends to be smaller than m_B. About 0.1 m.u. can be attributed to the larger relative bandwidth (RBW) of the SK response (by a factor of 1.5) as compared with that of the DD-1 response (Fig. 3). According to Bormann (2002b) the signal amplitude is roughly proportional to $RBW^{1/2}$. The main reasons for the systematically smaller m_b values, however, are the pronounced spectral saturation effect of short-period m_b, discussed in the introduction, and the short time window of 5 sec used at the CENC for m_b amplitude measurements, a value shorter than the average rupture duration of earthquakes with magnitudes >6. In contrast, Chinese broadband m_B, is measured at periods up to about 20 sec and within a time window of up to 60 sec. Accordingly, the difference $m_B - m_b$ growth with magnitude and may reach more than 1.5 m.u. (e.g., $m_B = 8.0$ and $m_b = 6.3$ for the Sumatra earthquake of 28 March 2005). For magnitudes of about 4, however, m_B and m_b are on average equal, because the rupture duration is then clearly less than 5 sec and both instrument responses record equally well maximum velocity amplitudes of seismic source spectra around corner frequencies of 1 Hz.

M_S-M_{S7}

Although M_S and M_{S7} are calculated from records with rather different responses (SK and 763, respectively; Fig. 3) and also employ different calibration functions, M_S and M_{S7} correlate best of all investigated relations (correlation coefficient $RXY = 0.9639$ with RMSO = ±0.1316 m.u.). Since $RXY = A_1/A_2$, SR1, SR2, and OR are almost identical and differ at the most 0.1 m.u. Because both magnitudes are determined down to 1° and 3°, respectively, values as low as 2.7 have been measured. On average, however, M_{S7} tends to be about 0.2 to 0.3 m.u. smaller than M_S, independent of magnitude. This is due to the previously mentioned constant offset of the M_S calibration function by +0.2 m.u. as compared with $\sigma(\Delta)$ of Vaněk *et al.* (1962), which is used for M_{S7} determinations between 20° and 160°.

M_{S7}-m_b and M_{S7}-m_B

M_{S7}-m_b shows saturation at m_b 7 and significantly larger scatter of m_b values (OR rotated closely toward SR1). In contrast, m_B does not saturate up to $m_B \approx 8$ and scales rather

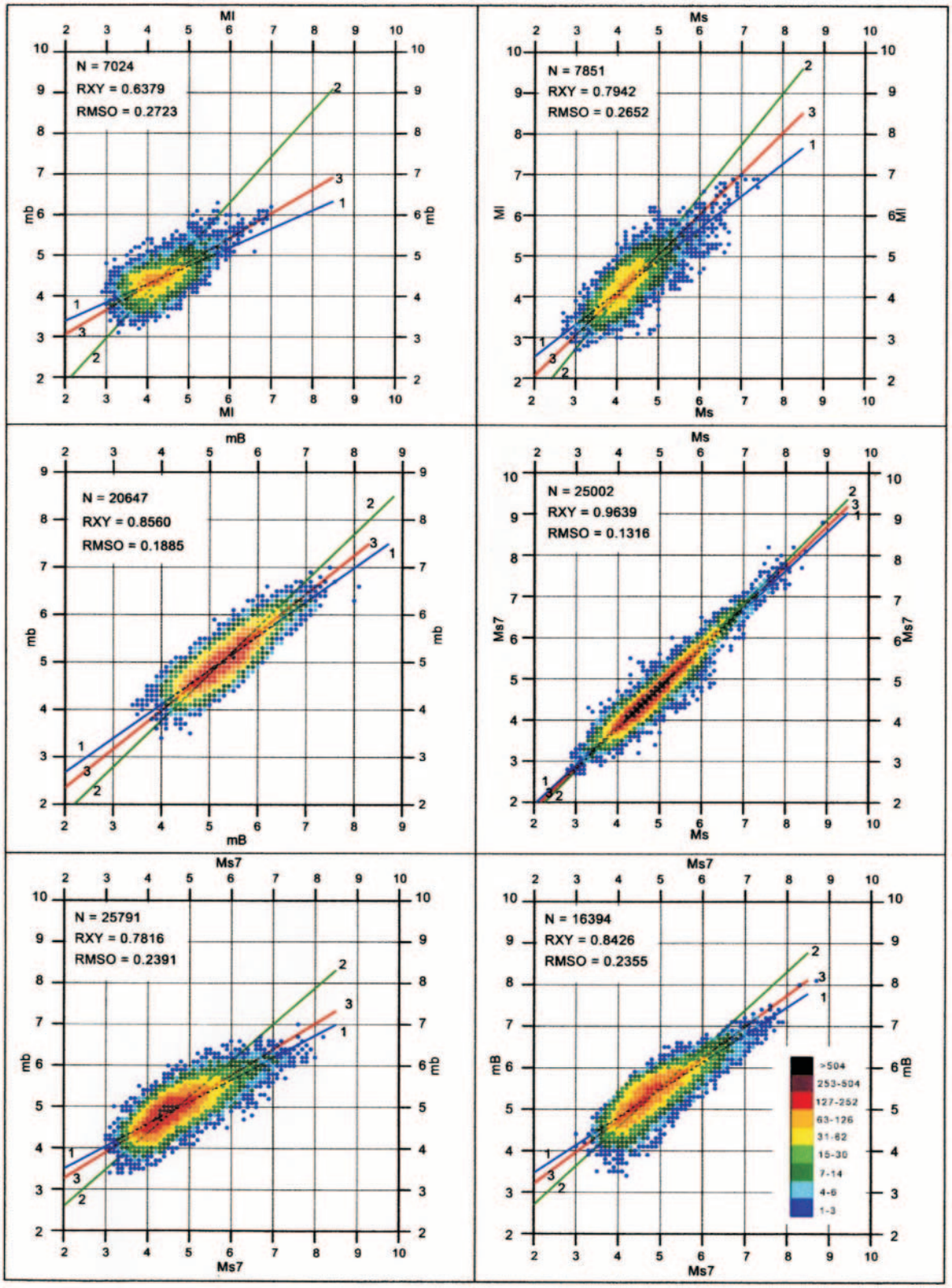

Figure 5. Standard regressions SR1 (blue line), SR2 (green line), and orthogonal regression OR (red line) for selected combinations of Chinese standard magnitudes. $RXY = A_1/A_2$, correlation coefficient; RMSO, standard deviation of the orthogonal errors; N, number of data pairs. The data frequency per data point has been color coded (see diagram lower right).

well and approximately linearly with M_{S7}. This illustrates the usefulness of broadband body-wave m_B for quick reliable estimates of the magnitude of strong earthquakes. Yet, because of distinct saturation of m_b, the related linear regressions with M_{S7} and M_S are reasonable approximations only for surface-wave magnitudes <7.

Comments on the Regression Relations for NEIC and Chinese Magnitudes

Figure 6 illustrates the relations between the most relevant NEIC and Chinese magnitudes.

m_b-m_b(NEIC)

This is the relationship with the most data (44,523). The correlation is rather high, the slope $A_1 = 1$ and the data scatter of the two short-period network magnitudes is comparable. However, there is a significant systematic difference between m_b and m_b(NEIC). For small values ($m_b \leq 4$) m_b(NEIC) is about 0.2–0.3 m.u. smaller than m_b. At such magnitudes the corner frequency of earthquake source spectra is usually at about or below 1 Hz. Related spectral amplitudes will be almost equally well recorded by the WWSSN short-period (SP), the USGS short-period PDE filter and the DD-1 response (compare Figs. 1 and 3). However, the WWSSN-SP and PDE-SP responses have only an RBW of about 1 to 1.6 octaves, whereas the DD-1 response has an RBW of 4.3 octaves. Accordingly, DD-1 amplitudes will be larger than those on WWSSN-SP or PDE-SP filtered records by a factor of about 1.6 to 2. This agrees with the 0.2 to 0.3 m.u. larger values of m_b as compared with m_b(NEIC) for low magnitudes. Yet, the China data set for m_b <4 also includes regional m_b data which may have a tendency to be larger than the corresponding teleseismic m_b (see previous discussion for M_L-m_b). The difference between m_b and m_b(NEIC) is reduced for magnitudes >4, is about zero between $m_b \approx 5$–6 and for m_b 7, m_b(NEIC) is on average about 0.3 m.u. larger. We see the reason for this in the greater measurement time windows applied at NEIC. This will, at medium magnitudes, first compensate for the bandwidth "advantage" of m_b as compared with m_b(NEIC) and then, for the strongest earthquakes, make m_b systematically smaller than m_b(NEIC).

m_B-m_b(NEIC)

The correlation is comparatively good as for m_B-m_b discussed previously. Again, for magnitudes of about 4, m_B and m_b(NEIC) are similar, because the periods around the corner frequency of source spectra at such magnitudes fall within the passband range of both types of records. However, for strong earthquakes, m_b(NEIC) will be smaller than m_B.

M_S-M_S(NEIC)

Both magnitudes correlate well and are on average identical for values of about 8 to 9. However, for magnitudes of about 4, resulting mostly from regional earthquakes, average M_S will be about 0.3 magnitude units larger than M_S(NEIC). This agrees with the distance-dependent errors of $M_S(20)$ at regional distances when calibrated with the IASPEI standard $\sigma(\Delta)$ function (Herak and Herak, 1993). The main reason for this discrepancy seems to be that for smaller-magnitude and regional earthquakes the A_{max} of surface waves usually occurs at $T < 18$ sec, thus yielding larger (A/T) ratios than those measured by NEIC at $T = 20 \pm 2$ sec. About 23% of the analyzed Chinese M_S data have been determined for events in $\Delta < 20°$, 11% were calculated for periods between 3 sec $\leq T <$ 10 sec and 76% for periods 10 sec $\leq T <$ 18 sec! Moreover, the systematically larger calibration values for M_S (+ 0.2 m.u), as compared with the IASPEI standard $\sigma(\Delta)$ function, may play a role in the discrepancy between M_S and M_S(NEIC).

M_{S7}-M_S(NEIC)

These data show the second best correlation. For measuring M_{S7} and M_S(NEIC), CENC and NEIC use instruments with identical response and within the distance range $20° \leq \Delta \leq 160°$ also the same IASPEI standard calibration function. In the magnitude range $3.5 < M_S < 9$ the two magnitudes differ by an average of no more than 0.1 m.u., although M_{S7} is calculated for periods 3 sec $\leq T <$ 30 sec. In fact, 45% of all M_{S7} magnitudes are measured at periods $T <$ 18 sec (down to 6 sec) and almost 20% at periods between 22 sec $< T <$ 30 sec.

M_S (NEIC)-m_b(NEIC) and M_S(NEIC)-m_B

Correlation coefficients and RMSO for both diagrams are almost the same as for M_{S7}-m_b and M_{S7}-m_B.

Summary, Conclusions, and Recommendations

Linear regression relationships have been derived to assess the relationship between China National Network magnitudes and NEIC magnitudes. They are suitable for comparing most types of magnitudes, with the exception of the relation between M_S and strongly saturating m_b. For a test set of teleseismic body and surface-wave magnitudes determined at CENC for the China National Network in a wide magnitude, period, and distance range, it was shown that the conditions for calculating linear regressions are reasonably met. Because the most suitable linear regression procedure depends both on the error ratio and the absolute errors of the correlated magnitudes, we have estimated these parameters from a Chinese test data set. With the values determined we proved that orthogonal regression is near to optimal for our data. Exceptions are M_S-m_b relations, for which SR1 is more suitable than OR.

From the comparison of NEIC and CENC magnitudes conclusions have been drawn with respect to the envisaged new IASPEI standards. Band-limited magnitudes such as

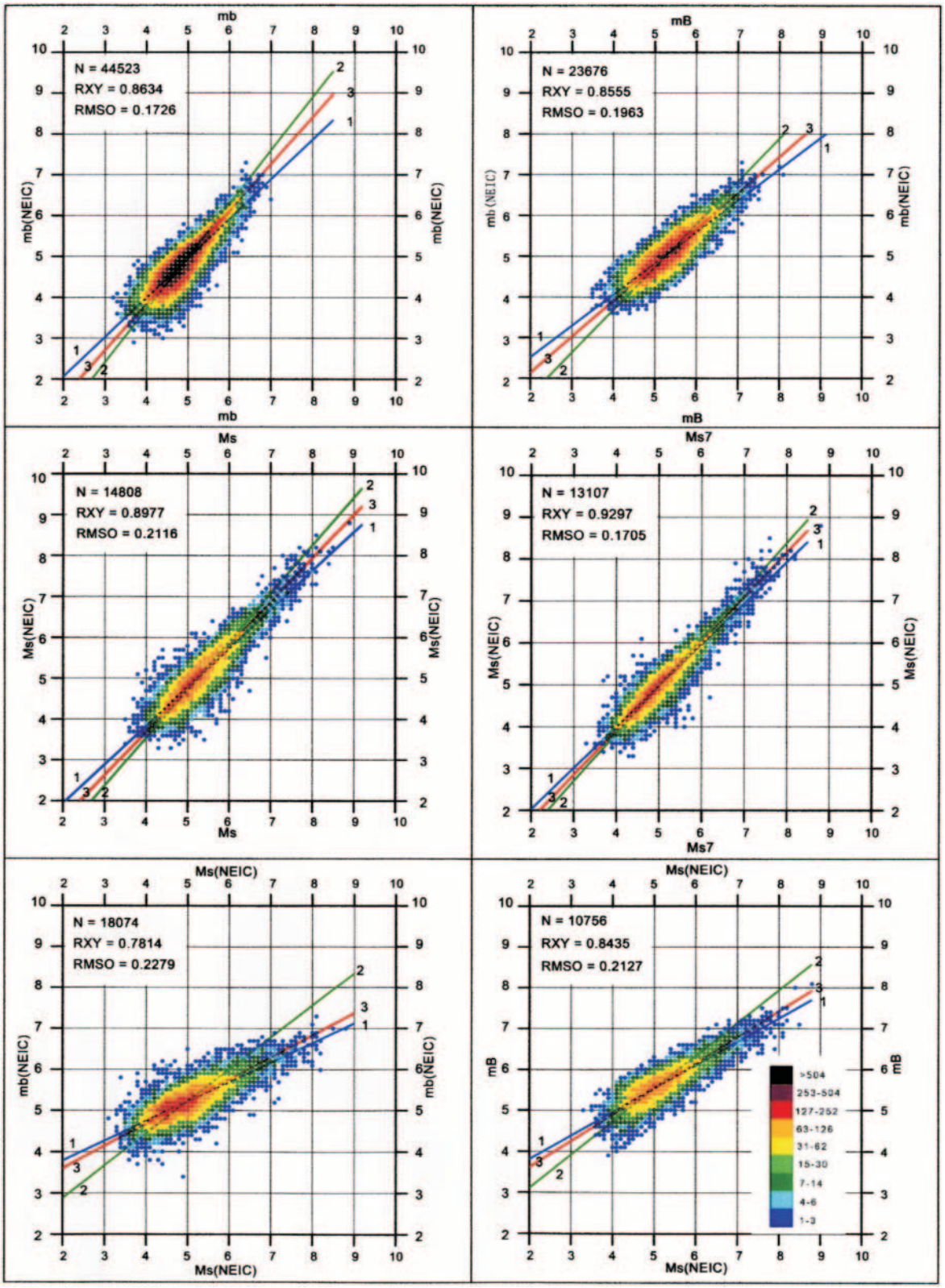

Figure 6. Standard regressions SR1 (blue line), SR2 (green line), and orthogonal regression OR (red line) for selected combinations of Chinese and NEIC magnitudes. $RXY = A_1/A_2$, correlation coefficient; RMSO, standard deviation of the orthogonal errors; N, number of data pairs. Color coding for data frequency classes is as in Figure 5.

M_S(NEIC) and m_b(NEIC) are the most widely determined and are now available for more than 40 years. Such data thus have some well-documented merits, for example, the combined consideration of band-limited M_S and m_b is effective in discriminating underground nuclear explosions from natural earthquakes (Marshall and Basham, 1972). The M_S/m_b is also a suitable hazard-relevant parameter, because it provides information about the relative amount of energy release in the high- and low-frequency ranges, which is relevant for seismic-hazard assessment. Moreover, Kaverina *et al.* (1996) revealed interesting relations of the so-called creepex parameter $c = M_S - am_b - b$ to earthquake-source geometry and tectonic origin. Thus, there is good reason to continue the tradition of determining M_S and m_b as established at NEIC and to also calculate these in the future. This is important for m_b, in particular, which for small earthquakes is often the only teleseismically measurable magnitude. However, we feel that especially m_b measurements would benefit greatly from a more rigorous standardization of the filter response and measurement time window applied. We have shown the effect of different window lengths by comparing m_b(NEIC) with m_b(CENC) and m_b(IDC), which may become larger than 1 m.u. for strong earthquakes. With respect to m_b determinations at distances $<20°$, we came to similar conclusions as NEIC from its own practice, that is, use of the Gutenberg–Richter $Q(\Delta,h)$—at least for short-period data—may not adequately estimate propagation effects at regional distances.

Accordingly, the current IASPEI WG on Magnitudes has recommended to the IASPEI Commission on Seismic Observation and Interpretation (CoSOI), to adopt short-period ($T < 3$ sec) body-wave magnitude m_b as a future standard within the distance range $21° \leq \Delta \leq 100°$, provided that the maximum *P*-wave ground amplitude within the entire *P*-phase train is measured on short-period WWSSN (or equivalently) filtered records.

When comparing $M_S(20)$ with a true velocity broadband M_S(BB), $M_S(20)$ tends to underestimate the surface-wave magnitude when $(A/T)_{max}$ occurs at periods below 18 sec. Although periods $T < 18$ sec are most frequently observed for regional earthquakes ($\Delta < 30°$), we have observed them both at the China and the German (GRSN) seismic networks far into the teleseismic distance range. Comparing $M_S(20)$ with Chinese M_S and M_{S7} we found systematic differences of the same order and tendency, because the latter are determined in a much wider range of periods and epicentral distances than $M_S(20)$ (see equations 3–5 and related text).

By comparing China broadband m_B with m_b determined at CENC and NEIC we note that m_B saturates much later (at about 8) and scales rather well and linearly with both China and NEIC surface-wave magnitudes. Therefore, we strongly recommend a reintroduction of broadband m_B into routine international seismological practice. Its determination should become a must for $m_b > 5$–5.5, when m_b begins to underestimate the *P*-wave magnitude (Fig. 5, middle-left). The performance of m_B is expected to be even better when the bandwidth of the recording system is enlarged in comparison with the China SK and 763 responses used at CENC for m_B determination. In this context, we also refer to a recent publication by Bormann and Wylegalla (2005) that indicates that summing up the velocity BB amplitudes of all major subevents in the *P*-wave train of very large earthquakes one can calculate a cumulative m_B (termed m_{Bc}), which scales well without saturation with M_w even for the largest earthquakes.

In agreement with our findings the IASPEI WG on Magnitudes has recommended to CoSOI to adopt a broadband surface-wave and body-wave magnitude, with the nomenclature M_S(BB) and m_B, respectively, as complementary international standards. The broadband velocity amplitudes (corrected by 2π) should be calibrated, as $M_S(20)$ and m_b, with the standard calibration function $\sigma(\Delta)$ according to Vaněk *et al.* (1962) and $Q(\Delta,h)_{PZ}$ by Gutenberg and Richter (1956). In contrast to $M_S(20)$, however, M_S(BB) will also cover the regional distance range, whereas the determination of m_B should, for the time being, be restricted to the same distance range as for m_b ($21° \leq \Delta \leq 100°$). However, one of us (P.B.) found for several recent regional earthquakes with $6.5 < M_W < 8$ in the distance range between 16° and 20° excellent agreement between m_B and M_w. Therefore, we encourage further investigations into the suitability of m_B determinations also at distances below 20°. In this context, we note that CENC also determines m_B for earthquakes at $100° < \Delta \leq 170°$ by using vertical-component amplitudes of *PP* waves and the respective Gutenberg–Richter *Q*-values. About 10% of the m_B values determined by the CENC are based on readings from *PP* waves and they agree well with those from *P* waves. Bormann and Khalturin (1975) showed that broadband m_B for *P* and *PP* waves, calibrated with their respective *Q*-values, scale ideally with an average difference of 0.05 m.u. and an RMSO of ± 0.15 m.u. only. This suggests that in the future *PP* waves should be considered as an acceptable additional candidate for m_B determinations, because they appear compatible with those from *P* waves and permit m_B determinations also in the core shadow of *P*.

The briefly mentioned recommendations of the IASPEI WG on Magnitudes have all been adopted by the CoSOI at the IASPEI General Assembly 2005 in Santiago de Chile. In addition standards for M_L and $m_b(L_g)$, the conversion of scalar seismic moment M_o in M_w, information on standards for nomenclature, etc., have been adopted. A detailed publication on these new standards is in preparation. Also, the International Seismological Centre (ISC) will be instrumental in disseminating the approved recommendations among seismological centers and in implementing them (ISC Newsletter July–December 2005). Parallel to this, in 2006, CENC and NEIC began to run parallel measurements of both their old and the newly recommended standards. The same is being done at the observatory CLL with data of the German Regional Seismic Network. Thus, new standard magnitude

data will soon be available, which will allow us to better test some of the preliminary findings and conclusions presented in this article.

Acknowledgments

We thank Siegfried Wendt of the Collm Observatory of the University of Leipzig for many fruitful discussions and partial contributions to this article, among them Figure 2. Special thanks go to James Dewey of the USGS NEIC. His critical reading of a first draft and very constructive suggestions helped us to better balance and focus the article on the issues relevant for the IASPEI WG on Magnitudes. We also thank Jochen Braunmiller, another anonymous reviewer, and Diane I. Doser, Associate Editor of *BSSA*, for their very helpful comments and suggestions. They helped in clarifying contents, shortening the text, eliminating typos, and improving grammar.

References

Aki, K. (1967). Scaling law of seismic spectrum, *J. Geophys. Res.* **72,** 1217–1231.

Bormann, P. (Editor) (2002a). *IASPEI New Manual of Seismological Observatory Practice*, Vols. 1 and 2, Geo ForschungsZentrum, Potsdam, 1250 pp.

Bormann, P. (2002b). Seismic signals and noise, in *IASPEI New Manual of Seismological Observatory Practice*, P. Bormann (Editor), Vol. 1, GeoForschungs Zentrum, Potsdam, Chapter 4.

Bormann, P., and V. I. Khalturin (1975). Relations between different kinds of magnitude determinations and their regional variations, in *Proceed. XIVth General Assembly of the European Seismological Commission*, Trieste, 16–22 September 1974. Nationalkomitee für Geodäsie und Geophysik, AdW der DDR, Berlin, 27–39.

Bormann, P., and K. Wylegalla (2005). Quick estimator of the size of great earthquakes, *EOS Trans. AGU* **86,** no. 46, 464.

Bormann, P., M. Baumbach, G. Bock, H. Grosser, G. I. Choy, and J. Boatwright (2002). Seismic sources and source parameters, in *IASPEI New Manual of Seismological Observatory Practice*, P. Bormann (Editor), Vol. 1, Geo Forschungs Zentrum, Potsdam, chapter 3.

Carroll, R. I., and D. Ruppert (1996). The use and misuse of orthogonal regression in linear errors-in-variables models, *Am. Stat.* **50,** no. 1, 1–6.

Castellaro, S., F. Mulargia, and Y. Y. Kagan (2006). Regression problems for magnitudes, *Geophys. J. Int.* **165,** 913–930.

Draper, N. R., and H. Smith (1998). Applied regression analysis, *Wiley Series in Probability and Statistics*, Third Ed., John Wiley, New York.

Fuller, W. A. (1987). *Measurement Error Models*, John Wiley, New York.

Granville, J. P., W.-Y. Kim, and P. G. Richards (2002). An assessment of seismic body-wave magnitudes published by the prototype International Data Center, *Seism. Res. Lett.* **73,** no. 6, 893–906.

Granville, J. P., P. G. Richards, W.-Y. Kim, and L. R. Sykes (2005). Understanding the differences between three teleseismic m_b scales, *Bull. Seism. Soc. Am.* **95,** no. 5, 1809–1824.

Guo, L., and M. Pang (1981). Surface-wave magnitude of earthquakes and its station Correction (in Chinese), *Acta Seism. Sinica* **3,** no. 3, 312–320.

Gutdeutsch, R., D. Kaiser, P. Bormann, R. Liu, and X. Ren (2005). Regressionsanalyse zur Umrechnung zwischen Magnituden des chinesischen Erdbebendienstes und des NEIC, Mitteilungen Nr. 3/2005 der Deutschen Geophysikalischen Gesellschaft, 14–22.

Gutenberg, B. (1945). Amplitude of surface waves and magnitude of shallow earthquakes, *Bull. Seism. Soc. Am.* **35,** no. 3, 3–12.

Gutenberg, B., and C. F. Richter (1956). Magnitude and energy of earthquakes, *Ann. Geofis.* **9,** no. 1, 1–15.

Herak, M., and D. Herak (1993). Distance dependence of M_S and calibrating function for 20 second Rayleigh waves, *Bull. Seism. Soc. Am.* **83,** no. 6, 1881–1892.

Kanamori, H. (1983). Magnitude scale and quantification of earthquakes, *Tectonophysics* **93,** 185–199.

Kaverina, A. N., A. V. Lander, and A. G. Prozorov (1996). Global creepex distribution and its relation to earthquake-source geometry and tectonic origin, *Geophys. J. Int.* **125,** 249–265.

Marshall, P. D., and P. W. Basham (1972). Discriminating between earthquakes and explosions employing an improved M_S scale, *Geophys. J. R. Astr. Soc.* **28,** 431–458.

Rezapour, M., and R. G. Pearce (1998). Bias in surface-wave magnitude M_S due to inadequate distance corrections, *Bull. Seism. Soc. Am.* **88,** no. 1, 43–61.

Richter, C. F. (1935). An instrumental earthquake magnitude scale, *Bull. Seism. Soc. Am.* **25,** 1–32.

Stromeyer, D., G. Grünthal, and R. Wahlström (2004). Chi-square regression for seismic strength parameter relations, and their uncertainties, with applications to an M_w based earthquake catalogue for central, northern and northwestern Europe, *J. Seism.* **8,** 143–153.

Vaněk, J., A. Zátopek, V. Kárnik, N. Kondorskaya, Y. Riznichenko, E. Savarenski, S. Solovév, and N. Shebalin (1962). Standardization of magnitude scales, *Bull. Acad. Sci. USSR, Geophys. Ser.* no. 2, (English translation), 108–111.

Willmore, P. L. (Editor) (1979). Manual of seismological observatory practice, World Data Center A for Solid Earth Geophysics, Report SE-20, September 1979, Boulder, Colorado, 165 pp.

GeoForschungsZentrum Potsdam (GFZ)
Division 2: Physics of the Earth
Telegrafenberg E423
D-14473 Potsdam, Germany
(P.B.)

China Earthquake Network Center
No. 63 Fuxing Avenue
Beijing 100036, People's Republic of China
(R.L., X.R.)

Institute for Meteorology and Geophysics
University of Vienna
Althanstrasse 14 UZA2
A 1090 Vienna, Austria
(R.G.)

Federal Institute for Geosciences and Natural Resources (BGR)
Stilleweg 2
30655 Hannover, Germany
(D.K.)

Università degli Studi di Bologna
Dipartimento di Fisica, Settore di Geofisica
v. le C. B. Pichat 8
40127 Bologna, Italy
(S.C.)

Manuscript received 30 March 2006.